Journal of Magnetic Resonance **136,** 1–5 (1999)
Article ID jmre.1998.1621, available online at http://www.idealibrary.com on IDEAL®

Stimulated Anti-Echo Selection in Spatially Localized NMR Spectroscopy

Jian-Ming Zhu,[1] and Ian C. P. Smith

Institute for Biodiagnostics, National Research Council of Canada, 435 Ellice Avenue, Winnipeg, MB, R3B 1Y6 Canada; and Departments of Chemistry and Physics, University of Manitoba, Winnipeg, MB, R3T 2N2 Canada

Received January 21, 1998; revised August 11, 1998

Spectral localization using the stimulated-echo acquisition mode (STEAM) is one of the most popular methods in volume-localized *in vivo* NMR spectroscopy. The localized volume signal is generated via stimulated echoes from spins excited by three 90° RF pulses, and the conventional STEAM sequence detects the stimulated-echo signal. From an analysis of the STEAM pulse sequence using the coherence transfer pathway formalism, stimulated anti-echoes are also formed by the same pulse sequence, which constitute the other half of the localized signal in the STEAM experiment. A new scheme of pulsed field gradients for the selection of stimulated anti-echoes was proposed, and localized spectroscopy in the stimulated anti-echo selection mode was achieved on a phantom and from *in vivo* rat brain.

Key Words: **stimulated anti-echo; STEAM; coherence pathway selection; pulse sequence.**

INTRODUCTION

Spatially localized *in vivo* NMR spectroscopy has evolved to a stage where clinical applications are being widely explored. Among many methods, spectral localization using direct volume excitation with selective RF pulses in the presence of magnetic field gradients is the most popular (*1–3*). Localized volume signals are usually generated as either stimulated echoes (STE) or double spin echoes (DSE) (*4*), depending on the pulse sequences used. The double-spin-echo localization method (PRESS) uses a sequence of 90°–180°–180° slice-selective RF pulses (*5, 6*), while in the stimulated-echo acquisition mode (STEAM) (*7–10*), a sequence of three 90° slice-selective RF pulses is applied. The STEAM sequence has the intrinsic disadvantage of losing half of the signal strength as compared to the double-spin-echo sequence with the same echo time. This imposes quite a limitation in localized spectroscopic *in vivo* applications, where the metabolites of very low concentration are of primary interest.

In this report, an analysis of the mechanism governing the half-signal loss in the stimulated-echo sequence is provided. This introduces a signal that was not selected and observed in the conventional STEAM experiment. This signal, named the stimulated anti-echo (STAE), constitutes the other half of the localized signals in stimulated-echo experiments. Using pulsed field gradients for coherence pathway selection, the detection of stimulated anti-echo signal was demonstrated in spatially localized NMR spectroscopy with phantom and *in vivo* experiments.

THEORY AND METHOD

Consider a general three-pulse sequence for volume localization,

$$\alpha(\phi_1)\text{–}\tau_1\text{–}\beta(\phi_2)\text{–}\tau_2\text{–}\gamma(\phi_3)\text{–}\tau_3\text{–}, \qquad [1]$$

where $\alpha(\phi_1)$, $\beta(\phi_2)$, and $\gamma(\phi_3)$ are three RF pulses with pulse phases ϕ_1, ϕ_2, and ϕ_3; τ_1, τ_2, and τ_3 are delays between RF pulses. The phase factors accumulated during the free precession between pulses are assumed to be: $\theta_1 = \omega_1\tau_1$, $\theta_2 = \omega_2\tau_2$, and $\omega_3 = \theta_3\tau_3$, which are generally caused by B_0 inhomogeneity and chemical shift differences, as well as field gradients applied for coherence pathway selection.

The observable terms of the density matrix for noninteracting, uncoupled $I = \frac{1}{2}$ spins, affected by all three RF pulses, can be expressed as

$$\begin{aligned}\sigma \propto\ & -iI_y\cos(2\phi_3 - 2\phi_2 + \phi_1 + \theta_1 - \theta_2 + \theta_3)\\ & \times (1 - \cos\gamma)\sin\alpha(1 - \cos\beta)/2\\ & + iI_x\sin(2\phi_3 - 2\phi_2 + \phi_1 + \theta_1 - \theta_2 + \theta_3)\\ & \times (1 - \cos\gamma)\sin\alpha(1 - \cos\beta)/2\\ & + iI_y\cos(-\phi_1 + \phi_2 + \phi_3 - \theta_1 + \theta_3)\sin\gamma\sin\alpha\sin\beta\\ & - iI_x\sin(-\phi_1 + \phi_2 + \phi_3 - \theta_1 + \theta_3)\sin\gamma\sin\alpha\sin\beta\\ & + iI_y\cos(\phi_1 - \phi_2 + \phi_3 + \theta_1 + \theta_3)\sin\gamma\sin\alpha\sin\beta\\ & - iI_x\sin(\phi_1 - \phi_2 + \phi_3 + \theta_1 + \theta_3)\sin\gamma\sin\alpha\sin\beta. \end{aligned} \qquad [2]$$

[1] To whom correspondence should be addressed at present address: Biomedical Magnetic Resonance Laboratory, University of Illinois at Urbana–Champaign, 2100 South Goodwin Avenue, Urbana, IL 61801. Fax: (217) 333-1133. E-mail: jzhu@uiuc.edu.

1090-7807/99 $30.00

TABLE 1
Signal Amplitude Dependence, Phase Factors, and Coherence Transfer Pathways (*P*) for the Observable Signals Generated by a General Three-Pulse Sequence

Signal	Amplitude dependence	Phase factors	*P*
DSE	$(1 - \cos\gamma)\sin\alpha(1 - \cos\beta)/2$	$2\phi_3 - 2\phi_2 + \phi_1 + \theta_1 - \theta_2 + \theta_3$	$(-1, 1, -1)$
STE	$\sin\gamma \sin\alpha \sin\beta$	$-\phi_1 + \phi_2 + \phi_3 - \theta_1 + \theta_3$	$(1, 0, -1)$
STAE	$\sin\gamma \sin\alpha \sin\beta$	$\phi_1 - \phi_2 + \phi_3 + \theta_1 + \theta_3$	$(-1, 0, -1)$

T_1 and T_2 relaxation effects are not considered here. The first two terms, representing the signal for the DSE, approach maximal amplitude when a combination of 90°–180°–180° pulse flip angles is used. The other four terms, representing the signals for the STE and STAE, respectively, reach maximal amplitude when an RF sequence of 90°–90°–90° pulse flip angles is applied. Each term also contains the coherence transfer pathway information, as indicated from the phase factors in the formula. Table 1 summarizes the amplitude dependence of RF pulse flip angles, the phase factors, and the coherence transfer pathways for these three types of observable signals. If three RF pulses are made slice selective, and applied in the presence of three orthogonal magnetic field gradients, these three types of echoes constitute the signals from the spins in the localized volume, since they are generated by the combined actions of all three slice-selection pulses. In localized spectroscopy, the localized DSE signal is generated via the PRESS sequence (*5, 6*), while the STE signal is obtained through the sequence known as STEAM, as well as other names (*7–10*). However, the presence of the localized stimulated anti-echo signal has not been previously demonstrated, and its application in spatially localized NMR has not been reported. This signal represents the other half-signal in the stimulated-echo pulse sequence, the loss of which results in the maximum attainable signal amplitude for the stimulated-echo method to be half that resulting from the double-spin-echo method, as shown in Eq. [2] and Table 1.

The selection of the double spin echo and stimulated echo in the localization sequence has been in principle straightforward, since a different combination of RF pulse flip angles can be used to maximize the signals. Furthermore, the timing delays between RF pulses and the spectral acquisition delay can be adjusted to capture only the desired localized echo signals in the acquisition window. In practice, however, the slice-selection pulses can never be made in such a uniform fashion that a clear separation can be made, since there are always slice profile effects and RF field inhomogeneities across the sample. This will cause significant contributions from undesired signals if no methods of coherence selection are applied.

This selection is based on the principle of coherence transfer pathway selection, and is conventionally achieved using phase cycling procedures (*11, 12*). For the purpose of localized *in vivo* spectroscopy, it is more beneficial to use pulsed field gradients for coherence pathway selection (*13, 14*), since the pulse sequences can be easily incorporated as the so-called "single-shot" experiments to minimize spectral artifacts caused from subtraction and addition errors. This will also enable localized volume shimming based on the same pulse sequence and from the same volume signal (*2*).

Considering specifically the selection of the STE and STAE signals from the 90°–90°–90° volume localization sequence,

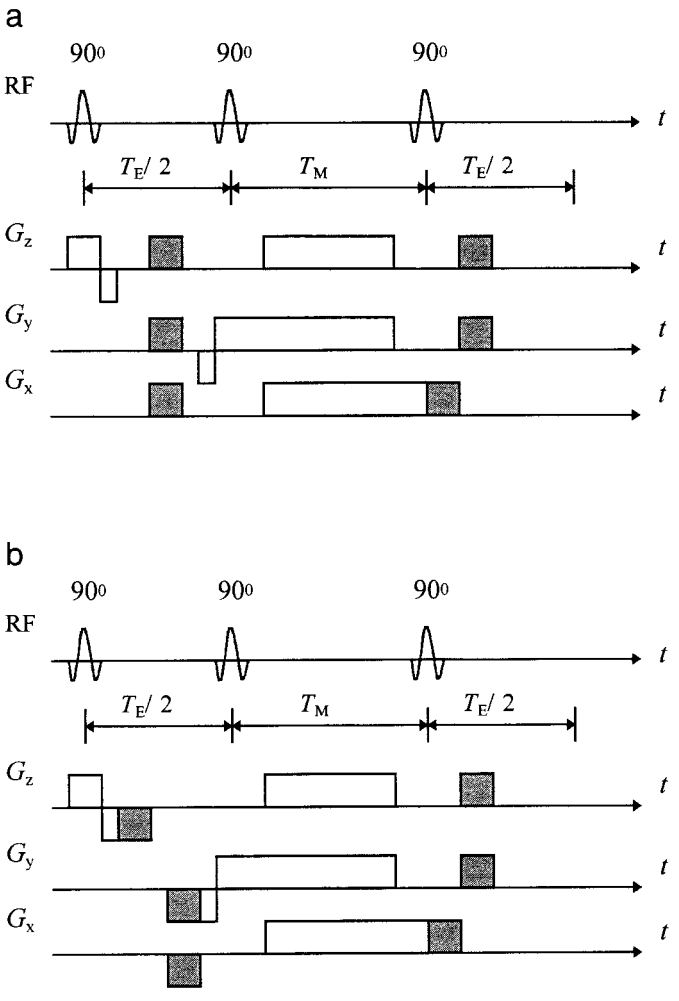

FIG. 1. Volume-localized spectroscopic sequences with (a) STE and (b) STAE selections. The difference in coherence pathway selection gradients is shown separately from slice-selection gradients, as highlighted by filled blocks.

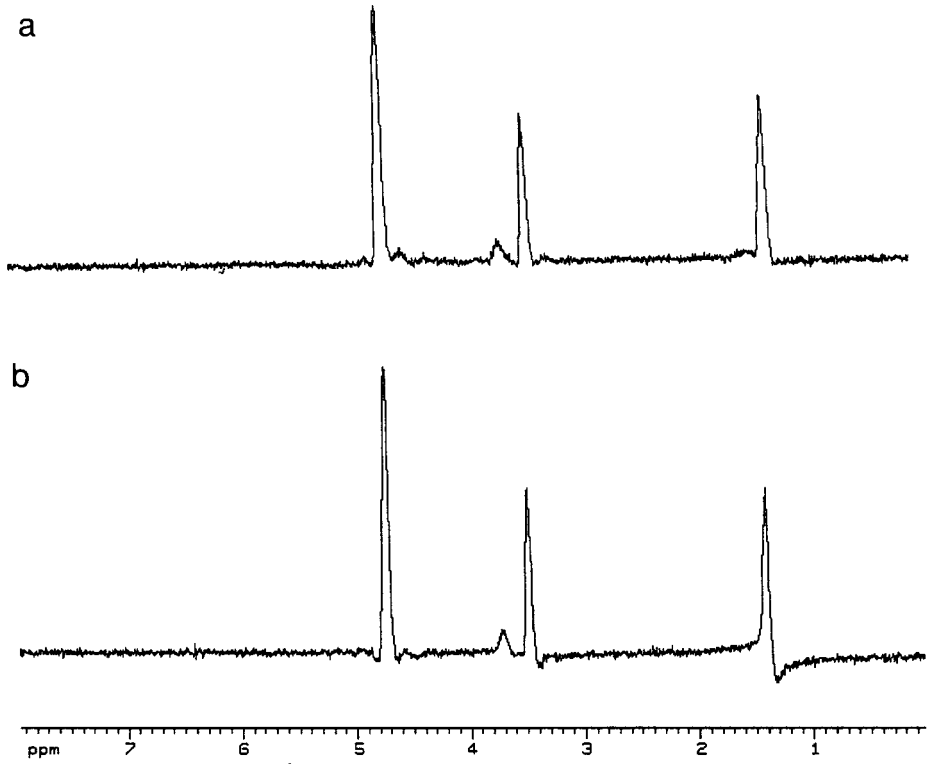

FIG. 2. Localized stimulated echo (a)- and anti-echo (b)-selected spectra using the pulse sequences in Fig. 1, acquired from a phantom containing 10 mM alanine (1.4, 3.75 ppm) and 10 mM glycine (3.5 ppm), dissolved in 99.9% D_2O, with a selected volume size of $6 \times 6 \times 6$ mm. The spectra were obtained with $T_E = 22$ ms, $T_M = 15$ ms, and 16 averages.

three pulsed gradients (G_1, G_2, G_3) are applied in each of three time-delay periods for coherence transfer pathway selection. From the condition for coherence transfer pathway selection (*14*),

$$p_1G_1 + p_2G_2 + p_3G_3 = 0, \qquad [3]$$

it is easy to derive that with a gradient ratio of $G_1{:}G_2{:}G_3 = 1{:}n{:}1$, the stimulated echo with the coherence pathway of $P = (1, 0, -1)$ can be selected. Similarly, the stimulated anti-echo can be selected using gradient ratio $G_1{:}G_2{:}G_3 = -1{:}n{:}1$, with the coherence pathway of $P = (-1, 0, -1)$. In Eq. [3], p_1, p_2, and p_3 are the coherence levels, and G_1, G_2, and G_3 are the field gradients applied during the three time-delay periods. The quantity n can be an arbitrary number, under the condition that complete dephasing of transverse magnetization is achieved by gradient G_2 during the mixing period.

For comparison, the three-90°-pulse localization sequence, combined with STE and STAE selections, is shown in Fig. 1. Three slice-selection pulses are applied in the presence of three mutually orthogonal field gradients, and the slice-selection gradients are accompanied by refocusing gradient lobes such that slice magnetization is refocused. With the addition of coherence-selection gradients, the refocusing gradient lobes can be placed in different time-delay periods, not necessarily following the frequency encoding gradients, with the condition that the above-mentioned gradient proportionality is kept for total gradients in the three time-delay periods.

RESULTS AND DISCUSSION

The pulse sequences for localized spectroscopy with STE and STAE selections were implemented on a 9.4-T Bruker Biospec system. The 21-cm-bore magnet is equipped with a custom-made, actively shielded field gradient coil from Magnex Scientific Ltd. (Abingdon, UK). Gradient strengths of up to 100 mT/m were used for slice and coherence pathway selection.

Experiments were demonstrated on a 25-ml cylindrical phantom containing 10 mM alanine and 10 mM glycine, dissolved in 99.9% D_2O. Figure 2 shows the absorption-mode experimental spectra from the localized STE and STAE volume signals, acquired with the pulse sequences shown in Fig. 1. The H_2O signal is set on resonance at 0 Hz. The spectra were acquired from a voxel of $6 \times 6 \times 6$ mm, with 16 acquisition averages, and were processed directly by Fourier transformation, without any line broadening or window function. Only first order phase correction was performed. Voxel shimming was achieved by optimizing field homogeneity using the H_2O

signal from a larger voxel with the same shape and at the same position.

Figure 2 shows that the stimulated anti-echo signal can indeed be generated experimentally from a localized volume, by means of a different gradient combination for coherence pathway selection, but with the same RF pulse sequence as the STEAM experiment. The two spectra from the STE and STAE selections have approximately the same peak intensities; however, there is a frequency-dependent phase shift in the STAE signal for off-resonance peaks, as clearly seen from the alanine CH_3 peak (1.4 ppm) and the glycine CH_2 peak (3.5 ppm). The intensities and phases of the STAE signal depend on the field homogeneity and on the difference between the resonance frequency and the carrier frequency. This is due to the fact that the effects of field inhomogeneity and chemical shifts are not "rewound" in the STAE selection, as shown in Table 1 from the accumulated phase factors—the exact same phenomena as gradient-echo selections in MRI experiments. The stimulated anti-echo can thus be considered to be T_2^* weighting during the echo time, as opposed to T_2 weighting for the stimulated-echo signal. There are also several reports of this chemical shift-dependent, phase-distortion phenomenon when implementing the localized STEAM experiment (*15–20*). It is probably due to the partial contribution from the localized STAE signals, where these two types of signals were not completely separated. Such stimulated anti-echoes are present with the stimulated echoes, but are conventionally eliminated in the STEAM experiments, which causes losing half of the volume signal from the localization sequence. The field homogeneity dependence was largely responsible for the failure to generate and observe STAE signals in spatially localized NMR. Coherence transfer anti-echoes have been reported in high-resolution experiments (*21, 22*) with high-field narrow-bore magnets where good field homogeneity can be easily achieved, and the anti-echo signals have been used in two-dimensional experiments for obtaining pure-phased 2D spectra (*13, 14*).

An *in vivo* demonstration of this STAE selection experiment was performed on live rat brain, along with localized STEAM spectroscopy. Figure 3 presents localized *in vivo* spectra obtained with STEAM- and STAE-selected sequences from the same voxel (size 3 × 3 × 3 mm) on a live rat brain. Water suppression was achieved using the conventional CHESS sequence. It clearly indicates that STAE-selected localized spectroscopy is also achievable even *in vivo.* However, due to larger tissue susceptibility differences present *in vivo*, the line broadening effect in the STAE-selected spectrum is more serious, as can be noted from Fig. 3b.

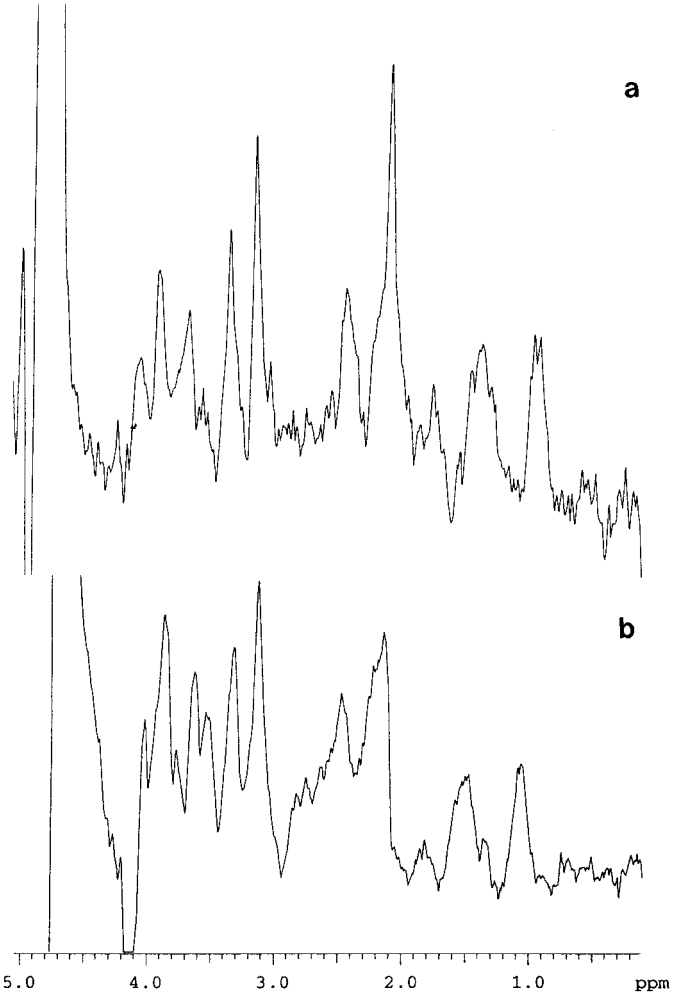

FIG. 3. Water-suppressed *in vivo* proton spectra acquired from a voxel of 27 ml, localized in a rat brain using (a) stimulated-echo selection and (b) stimulated anti-echo selection with the pulse sequence shown in Fig. 1. The spectra were obtained with T_E = 15 ms, T_M = 15 ms, and 256 averages. The linewidths of the resonances are broader in the STAE-selected spectrum due to tissue susceptibility effects, particularly, the NAA peak at 2.1 ppm.

CONCLUSION

This report, for the first time, demonstrated the presence and observation of stimulated anti-echo signals in spatially localized NMR experiments, which provided a further understanding of the stimulated-echo sequence and its associated mechanism of half-signal loss as compared to the double-spin-echo experiment. A particular sequence of pulsed field gradients, based on the principle of coherence pathway selection, leads to selective detection of the STAE signal. This signal, not conventionally selected in the stimulated-echo experiment, accounts for the other half lost echo signal. Experiments were demonstrated in the context of localized spectroscopy.

Devising a new method of coherence transfer pathway selection, to detect both localized signals simultaneously from the STEAM sequence, should lead to double the localized signal. This stimulated anti-echo signal should also find important applications in imaging experiments, similar to gradient echo-selected MRI experiments. These will be subjected to further studies.

ACKNOWLEDGMENTS

Financial support from the Natural Sciences and Engineering Research Council of Canada and the National Research Council of Canada is gratefully acknowledged.

REFERENCES

1. M. Decorps and D. Bourgeois, Localized spectroscopy using static magnetic field gradients, *in* "NMR Basic Principles and Progress" (P. Diel, E. Fluck, H. Gunther, R. Kosfeld, and J. Seelig, Eds., and M. Rudin, Guest Ed.), Vol. 27, Springer-Verlag, Berlin (1992).
2. J. R. Alger, Spatial localization for in vivo magnetic resonance spectroscopy: Concepts and commentary, *in* "NMR in Physiology and Biomedicine" (R. Gillies, Ed.), Academic Press, New York (1994).
3. R. Gruetter and C. Boesch, *Q. Magn. Reson. Biol. Med.* **2,** 99 (1995).
4. E. L. Hahn, *Phys. Rev.* **80,** 580 (1950).
5. P. A. Bottomley, U.S. Patent 4480228 (1984).
6. P. A. Bottomley, *Ann. N.Y. Acad. Sci.* **508,** 333 (1987).
7. J. Granot, *J. Magn. Reson.* **70,** 488 (1986).
8. R. Kimmich and D. Hoepfel, *J. Magn. Reson.* **72,** 379 (1987).
9. J. Frahm, K.-D. Merboldt, and W. Hanicke, *J. Magn. Reson.* **72,** 502 (1987).
10. J. J. van Vaals, A. H. Bergman, J. H. den Boef, H. J. van den Boogert, and P. H. J. van Gerwen, *Magn. Reson. Med.* **19,** 136 (1991).
11. J. Keeler, *in* "Multi-nuclear Magnetic Resonance in Liquids and Solids—Chemical Applications" (P. Granger and R. K. Harris, Eds.), NATO ASI Series C, Vol. 322, pp. 103–129, Kluwer, Dordrecht, The Netherlands (1990).
12. D. L. Turner, Phase cycling, *in* "Encyclopedia of NMR" (D. M. Grant and R. K. Harris, Eds.), Wiley, New York (1996).
13. J. Keeler, R. T. Clowes, A. L. Davis, and E. D. Laue, *in* "Methods in Enzymology" (J. Oppenheimer and T. L. James, Eds.), Vol. 239, Academic Press, San Diego (1994).
14. J.-M. Zhu and I. C. P. Smith, *Concepts Magn. Reson.* **7,** 281 (1995).
15. L. Bolinger, R. E. Lenkinski, and J. S. Leigh, *SMRM Abstracts* **9,** 1330 (1990).
16. P. B. Kingsley and J. S. Taylor, *SMRM Abstracts* **10,** 3814 (1992).
17. W. Zhang and P. van Hecke, *J. Magn. Reson.* **91,** 408 (1991).
18. D. Ballon, M. Garwood, and J. A. Koutcher, *Magn. Reson. Imaging* **9,** 569 (1991).
19. G. S. Payne and M. O. Leach, *Magn. Reson. Imaging* **13,** 629 (1995).
20. R. V. Mulkern, J. L. Bowers, S. Peled, and D. S. Williamson, *J. Magn. Reson. B* **110,** 255 (1996).
21. T. H. Mareci and R. Freeman, *J. Magn. Reson.* **48,** 158 (1982).
22. R. R. Ernst, G. Bodenhausen, and A. Wokaun, "Principles of Nuclear Magnetic Resonance in One and Two Dimensions," Clarendon Press, Oxford, UK (1987).